AD-A252 103

OFFICE OF NAVAL RESEARCH

GRANT N00014-91-J-1667

R&T Code 4131061

Technical Report No. 1

Diffusive Transport of the Hydrated Electron: A Pseudoclassical Model

by

Gabriela S. Del Buono, Peter J. Rossky,
and Tim H. Murphrey

DTIC
ELECTE
JUN 16 1992
S B D

Prepared for Publication

in

The Journal of Physical Chemistry

Department of Chemistry and Biochemistry
The University of Texas at Austin
Austin, Texas 78712

January 29, 1992

Reproduction in whole or part is permitted for any purpose of the United States Government.

This document has been approved for public release and sale; its distribution is unlimited.

92-15238

92 6 16 010

REPORT DOCUMENTATION PAGE

Form Approved
OMB No. 0704-0188

Public reporting burden for this collection of information is estimated to average 1 hour per response, including the time for reviewing instructions, searching existing data sources, gathering and maintaining the data needed, and completing and reviewing the collection of information. Send comments regarding this burden estimate or any other aspect of this collection of information, including suggestions for reducing this burden, to Washington Headquarters Services, Directorate for Information Operations and Reports, 1215 Jefferson Davis Highway, Suite 1204, Arlington, VA 22202-4302, and to the Office of Management and Budget, Paperwork Reduction Project (0704-0188), Washington, DC 20503

1. AGENCY USE ONLY *(Leave blank)*

2. REPORT DATE
1992

3. REPORT TYPE AND DATES COVERED
Technical Report, Interim, 4/1/91 - 5/31/92

4. TITLE AND SUBTITLE
Diffusive Transport of the Hydrated Electron: A Pseudoclassical Model

5. FUNDING NUMBERS
Grant #: N00014-92-J-1667
R&T Project #: 4131061---01

6. AUTHOR(S)
Gabriela S. Del Buono, Peter J. Rossky and Tim H. Murphrey

7. PERFORMING ORGANIZATION NAME(S) AND ADDRESS(ES)
Department of Chemistry and Biochemistry
The University of Texas at Austin
Austin, Texas 78712

8. PERFORMING ORGANIZATION REPORT NUMBER
NR-1

9. SPONSORING/MONITORING AGENCY NAME(S) AND ADDRESS(ES)
Office of Naval Research
800 North Quincy Street, Code 1113PS
Arlington, VA 22217-5000

10. SPONSORING/MONITORING AGENCY REPORT NUMBER

11. SUPPLEMENTARY NOTES
The Journal of Physical Chemistry (in press, 1992)

12a. DISTRIBUTION/AVAILABILITY STATEMENT
This document has been approved for public release and sale; distribution of this document is unlimited.

12b. DISTRIBUTION CODE

13. ABSTRACT *(Maximum 200 words)*
In order to elucidate the factors responsible for the enhanced diffusion rate of the hydrated electron compared to halide ions, a pseudoclassical simulation technique that mimics the adiabatic dynamical response of the electron is applied to halide-like ions in water for different solute-solvent potential models. Both the adiabatic and classical diffusive behavior are evaluated and compared to the quantum dynamics of the hydrated electron. It is shown that the adiabatic response *per se* is essential, but only partially responsible for the diffusion rate enhancement of the excess electron. Specific features of the solute-solvent interaction potential must also be taken into account for a realistic description of the electron mobility. These include the nature of the short range repulsion associated with the spatial confinement of the excess electron and the partial penetration of the excess electronic distribution into the first hydration shell. When these effects are also incorporated into the pseudoclassical model, both the solvated electron dynamics and solvation structure are closely reproduced by the model system.

14. SUBJECT TERMS
solvated electron, diffusion, simulation

15. NUMBER OF PAGES
41

16. PRICE CODE

17. SECURITY CLASSIFICATION OF REPORT	18. SECURITY CLASSIFICATION OF THIS PAGE	19. SECURITY CLASSIFICATION OF ABSTRACT	20. LIMITATION OF ABSTRACT
Unclassified	Unclassified	Unclassified	UL

JP92 0222M
Revised 4/28/92

DIFFUSIVE TRANSPORT OF THE HYDRATED ELECTRON: A PSEUDOCLASSICAL MODEL

Gabriela S. Del Buono, Peter J. Rossky*
and Tim H. Murphrey

Department of Chemistry and Biochemistry
The University of Texas at Austin

Austin, Texas 78712

ABSTRACT

In order to elucidate the factors responsible for the enhanced diffusion rate of the hydrated electron compared to halide ions, a pseudoclassical simulation technique that mimics the adiabatic dynamical response of the electron is applied to halide-like ions in water for different solute-solvent potential models. Both the adiabatic and classical diffusive behavior are evaluated and compared to the quantum dynamics of the hydrated electron. It is shown that the adiabatic response *per se* is essential, but only partially responsible for the diffusion rate enhancement of the excess electron. Specific features of the solute-solvent interaction potential must also be taken into account for a realistic description of the electron mobility. These include the nature of the short range repulsion associated with the spatial confinement of the excess electron and the partial penetration of the excess electronic distribution into the first hydration shell. When these effects are also incorporated into the pseudoclassical model, both the solvated electron dynamics and solvation structure are closely reproduced by the model system.

DTIC COPY INSPECTED

Accession For
NTIS GRA&I ☑
DTIC TAB ☐
Unannounced ☐
Justification

By
Distribution/
Availability Codes
Dist | Avail and/or Special
A-1

I INTRODUCTION

The dynamics of ions in solution is a topic of wide chemical and biological importance. Familiar examples include ionic diffusion in solution, the transport of ions across membranes, and ionic dynamics in polyionic systems, such as biopolymers. An accurate molecular description of these and other inhomogeneous systems is predicated on a detailed understanding of the dynamics of ions in bulk solutions. One of the most interesting ionic systems in terms of its basic physics is the hydrated electron (e^-_{aq}), which was discovered more than two decades ago.[1] Since then, the structure and dynamics of this system have been intensively studied both experimentally and theoretically.

Several models of electron solvation have been proposed. Currently, both experiments and computational studies support the so-called cavity model,[2] which is based on the idea that the roughly spherical excess electronic wavefunction is solvated in an ion-like manner. Thus, the excess electron ground state distribution is localized in a cavity surrounded by shells of the solvent, with those in the inner shell exhibiting preferential OH bond orientation with respect to the center of the electron distribution in the cavity.[2]

Despite the similar solvation characteristics, the hydrated electron exhibits a relatively high diffusion rate in relation to its ionic counterparts (about 2-3 times higher). This specific property of the solvated electron has been the subject of considerable theoretical speculation and modelling.[2–6]

Transport mechanisms involving tunneling through potential barriers, adiabatic hopping over large distances, and even Grotthuss-type diffusion mechanisms have been invoked in an attempt to explain the relatively high mobility of excess electrons in liquid water.[2–4] However, recent simulation studies employing adiabatic dynamics,[5,6] found that long-range hopping does not occur, and suggest that in the case of electron diffusion in water, migration is predominantly polaronic in nature. Similar conclusions appear to apply to the ammoniated electron.[7]

The origin of the enhanced electronic diffusion coefficient was attributed to fundamental differences in the dynamics of electrons and classical ions.[5] It was argued that in the electronic system, the charge distribution which polarizes the local molecular solvation environment is capable of instantaneously responding to changes in the local solvent configuration, resulting in rapid variation of the solvated electron spatial density. In contrast, classical halide ions are incapable of instantaneously responding to local solvent fluctuations due to inertial effects. For this inertial case, a restoring force would be provided by the ionic source, causing the solvent to tend to return more closely to its initial configuration than it would in the electronic case. Nevertheless, this hypothesis as to the origin of the enhanced diffusion rate has never been demonstrated. One cannot rule out important alternative contributions to the dynamics associated with differences in the short-ranged interactions between solute and solvent.

In order to examine the contribution of such variations in interactions, one

must examine the dynamical response of the system to these changes. However, in accord with the reasoning above, present analytical theories of ion dynamics in solution[8] cannot be expected to explain the diffusive behavior of the solvated electron. On the other hand, computer simulation of alternative pseudoclassical models are readily accessible. The precise algorithm used to implement this concept will be described in the next section.

We will explore ionic motion governed by what we will refer to as "adiabatic" ion dynamics simulations. In such simulations, the otherwise classical ion responds instantaneously to changes in solvent configuration and lacks a classical inertial component in its dynamics. Different ion-solvent interaction potentials will also be studied, and the results will be compared to analogous classical MD simulations, as well as to quantum simulation results for e^-_{aq}. The comparative results will be used to delineate the features critical to the observed diffusive transport of the solvated electron.

In Section II, we give the details of our computer simulations. Section III outlines the different potential functions utilized. The results are presented and discussed in Section IV. Though our emphasis is on dynamical properties of the solute, some structural characteristics and energetics resulting from the different models studied are also included in order to complete the comparison between electron and pseudoclassical ion simulations. In Section V, we summarize the results and present our conclusions.

II COMPUTATIONAL METHODS

In this section, we describe the simulation protocol and algorithms.

A Classical molecular dynamics simulations

Standard molecular dynamics simulations of one bromide ion and 500 SPC[9] water molecules confined to a cubic box under periodic boundary conditions are performed. The SPC model is chosen to be consistent with our earlier work.[5] In particular, the model Hamiltonian previously developed for treating the quantum electron is specifically designed to be compatible with the SPC model for water. The size of the cubic cell (24.66 $\mathring{A}$) is chosen to obtain a molecular density of 0.0333 molecules/$\mathring{A}^3$. The equations of motion are integrated with a time step of 2 femtoseconds using the Verlet algorithm combined with the SHAKE algorithm[10] in order to satisfy the constraints associated with the rigid water molecules. Long-range interactions are calculated via the Ewald summation method.[11] The particular motivations for the use of the Ewald sum are discussed below.

For each of the cases studied, the system was allowed to equilibrate for about 40 picoseconds before production runs were performed; Table I shows the actual length of each simulation. Every tenth configuration was stored for analysis.

B Adiabatic molecular dynamics simulations

For adiabatic *quantum* MD simulations, the time evolution of the system is calculated within the Born-Oppenheimer approximation, so that the solvent dynamics is followed on the electronic ground state potential energy surface.[5] In our adiabatic MD simulations, this behavior is mimicked by placing the ion at the *minimum* of its interaction potential after each timestep of solvent dynamics. A new solvent configuration is then obtained by solving the classical equations of motion, accounting for the forces exerted by the ion as well. A new position for the ion at the potential minimum is subsequently calculated, and so on.

The ionic potential minimum is found by first performing steepest descent[12] for a fixed solvent configuration to obtain an approximation. These coordinates are further refined using the Polak-Ribiere version of the conjugate gradient methods.[12,13] For the steepest descent and conjugate gradient methods one desires a smooth potential energy surface.[14] To this end, the long-range interactions were calculated using Ewald summation to avoid discontinuities in the energy and its gradient, as would appear in other approaches such as those employing spherical truncation.

The conservation of energy by the adiabatic dynamics procedure outlined here is easily demonstrated. The time derivative of the expression for the total energy E of the system must vanish. Formally, the total energy of a classical ion-water system is,

$$E = \frac{1}{2}m_I\dot{\mathbf{r}}_I^2 + \sum_\alpha \frac{1}{2}m_\alpha\dot{\mathbf{r}}_\alpha^2 + V_W(\mathbf{r}_W) + V_I(\mathbf{r}_W, \mathbf{r}_I),$$

where $m_I, \dot{\mathbf{r}}_I, \ddot{\mathbf{r}}_I$ are the mass, velocity and acceleration of the ion, and $m_\alpha, \dot{\mathbf{r}}_\alpha, \ddot{\mathbf{r}}_\alpha$ are the mass, velocity and acceleration of each one of the water molecule sites α. V_W and V_I are the solvent-solvent, and ion-solvent interaction potentials respectively.

The time derivative of the energy is,

$$\frac{dE}{dt} = m_I\dot{\mathbf{r}}_I.\ddot{\mathbf{r}}_I + \nabla_I V_I.\dot{\mathbf{r}}_I + \sum_\alpha [m_\alpha\dot{\mathbf{r}}_\alpha.\ddot{\mathbf{r}}_\alpha + (\nabla_\alpha(V_W + V_I).\dot{\mathbf{r}}_\alpha)].$$

For Newtonian dynamics, substitution of the accelerations by the following expressions,

$$\ddot{\mathbf{r}}_\alpha = -\frac{1}{m_\alpha}\nabla_\alpha V_{total}$$

$$\ddot{\mathbf{r}}_I = -\frac{1}{m_I}\nabla_I V_{total},$$

cancels out both the ionic and water terms of the energy derivative expression yielding a vanishing result. Using adiabatic dynamics for the ion, $\dot{\mathbf{r}}_I = 0$ and $\nabla_I V_I = 0$, so that the time derivative of the energy vanishes in this case as well.

All simulation conditions were chosen to be exactly the same as the classical MD cases. The starting configurations were obtained from the respective classical simulations, and used to equilibrate the systems.

C Quantum molecular dynamics simulations

For purposes of comparison, a Quantum Molecular Dynamics simulation of the excess electron in water was performed, analogous to that previously reported from this laboratory.[5]

The algorithm, as well as the electron-water pseudopotential utilized, are presented in Ref.15; the only modification we made to the algorithm is the implementation of the Ewald method to calculate long-range interactions, instead of using spherical truncation. This was done to preserve, as far as is possible, equivalent conditions for all ion-water systems considered in this study.

III SOLUTE-WATER PAIR POTENTIALS

Our goal in this study is to delineate the properties of the system that are responsible for the enhanced diffusion rate of the electron compared to simple atomic ions. One contribution already discussed is a difference in dynamical response. However, differences in the solute-solvent interaction potential must also be considered. As will be seen below, these differences are also essential.

In this section, we describe three models considered as caricatures of the solvated electron.

From previous path integral studies,[16,17] it is known that the size of the simulated e^-_{aq} solute is comparable to that of a halide ion, with a radius

intermediate between Cl^- and Br^-. In addition to the structural features of solvation, e^-_{aq} roughly resembles Br^- in terms of their solute-solvent energies; therefore, we use Br^- as our reference solute for this study.

Each one of the three electron-water pair potentials studied incorporates a set of characteristics deemed potentially significant in an attempt to mimic the electronic behavior in water. The parameters corresponding to each model are given in Table II. Figure 1 shows the values of the total pair potential for geometries with the ion center collinear with either the OH bond direction (Fig.1a) or the HOH bond angle bisector (Fig.1b).

A Model 1

The first potential function studied is of a simple Lennard-Jones ion type. The ion is represented by a negative point charge, and the Lennard-Jones parameters used are those given by Heinzinger.[18]

An important limitation of Model 1 results from the fact that the effective short range interaction between the solvent and the solute is fundamentally different for Br^- and e^-_{aq}. For the halide, the electronic distribution is relatively rigid (being determined by the ionic nucleus), so that a rapidly varying and strong repulsion exists when the solute and solvent wavefunctions overlap. For the electron, the distribution is determined only by the solvation structure, so that one expects a balance between the alternative energetic costs of interpenetration and confinement of the excess electron.

In the following two models (Models 2 and 3), we assume as a guiding

concept the simple view that the distance dependence of the solute-solvent potential arises from confinement alone. The premise is that the degree of electronic interpenetration is not strongly dependent on center of mass separation.

B Model 2

The second potential examined is comprised of a simple Coulombic term identical to that used in the first potential, and a "soft" repulsive potential. This latter, nonelectrostatic, portion of the ion-water interaction is described using a repulsive term of the form:

$$\frac{A}{Br^2 + C\exp(\alpha r)} + D\exp(-\beta r^2), \tag{1}$$

$$A, B, C, D, \alpha, \beta > 0.$$

The motivation for choosing this functional form and the values of the parameters listed in Table II are as follows:

* The position of the pair potential minimum is chosen to coincide with that of Model 1, the Coulomb + Lennard-Jones potential ($r_{min} = 3.32\mathring{A}$), for the bond oriented approach.

* The potential should mimic the quite different repulsion between water and an excess electron compared to an atomic ion described above. If we think about this in terms of a particle in a box, the molecules surrounding the quantum particle would be the determinants of the box size. As the

energy is proportional to the inverse square of the linear dimension of this box, we are led, at relatively small bromide-water distances, to a form varying as $\frac{1}{r^2}$.

* At bromide-water distances beyond the first solvation shell, the potential should decay rapidly; this feature is needed to maintain a short-ranged repulsive interaction. We accomplish this via the exponential in the denominator of the first term in Eq.(1).

* The second term in the potential function becomes significant only at very small ion-solvent distances, and is added to ensure that the potential maximum is high enough to allow practical implementation along with a (singular) Coulombic term.

C Model 3

The third potential studied here includes also a modified Coulomb interaction superimposed on a soft repulsive potential of the type introduced in Model 2. The modification of the Coulomb potential used is designed to more realistically describe the electrostatics associated with the distributed electronic charge. The corresponding repulsive term is then adjusted somewhat to produce a potential which has comparable strength.

It has been shown that the ground state of an excess electron in polar solvents is a bound state.[2b] The typical ground-state wavefunction in water resembles, to a good approximation, a Gaussian distribution.[19] It is also known that the tail of the electronic wavefunction does penetrate the first

shell of water molecules around the electron. Using our pseudoclassical model we can introduce this effect by representing the ion as a Gaussian charge distribution, instead of a simple point charge. The electron density, $\rho(\mathbf{r})$, is given by

$$\rho(\mathbf{r}) = q\left(\frac{1}{2\pi\xi^2}\right)^{\frac{3}{2}} \exp\left(-\frac{\mathbf{r}^2}{2\xi^2}\right),$$

where ξ is the width of the Gaussian.

The value of the width used here is based on the average radii of the electronic wavefunction obtained from previous path integral studies,[19]

$$< \int \rho(\mathbf{r})|\mathbf{r}|d\mathbf{r} >= 1.88\mathring{A}$$

$$< \int \rho(\mathbf{r})\mathbf{r}^2 d\mathbf{r} >^{\frac{1}{2}} = 2.05\mathring{A}.$$

From these two equations, ξ is estimated to be $1.18\mathring{A}$.

The parameters for the repulsive part of the potential are modified slightly to reproduce the potential described in Section IIIB near the minimum for the bond oriented approach (see Table II). In this case, the $\exp(-\beta r^2)$ factor is not needed.

The final potential function is given by,

$$V(\mathbf{r}) = \frac{q(Br^-)q(H_2O site)}{\mathbf{r}} erf\left(\frac{\mathbf{r}}{\sqrt{2}\xi}\right) + \frac{A}{B\mathbf{r}^2 + C\exp(\alpha\mathbf{r})},$$

where $erf(x)$ is the error function.

We note that the introduction of the solvent penetration of the electronic distribution only for the purpose of evaluating the electrostatic forces

is reasonable *only* if the energetic contribution due to the electronic interpenetration is not very dependent on the configuration of molecules in the first solvation shell.

Further, we must emphasize that Model 2 and Model 3 make explicit and implicit use of knowledge about the structure of hydrated electron. Hence, they are not intended to be *a priori* models, and, for example, are only potentially pertinent at ambient temperature and solvent density. This aspect is discussed further in the Conclusions.

As can be seen in Fig.1, the pair potentials for the three models differ significantly. In particular, both Models 2 and 3 show considerably less short ranged repulsion than Model 1, by design, although both also manifest somewhat shallower absolute binding. It is especially interesting to note the relatively large difference in angular dependence between Model 2, the point charge model, and Model 3, the model incorporating electronic penetration.

IV RESULTS AND DISCUSSION

In this section, we compare and contrast the results of the classical and adiabatic simulations of the hydrated bromide ion and those of the e^-_{aq} simulations.

Various dynamical properties of each species are examined to determine the effects of different interaction potentials on ion mobility.

This information is then used to infer the features critical to transport for the hydrated electron. Structural and energetical properties of the systems

are also presented as complementary information in order to obtain a better understanding of the character of the different models.

A Diffusion

In a molecular dynamics simulation, the self-diffusion coefficient D of a particle may be calculated in at least two ways. The first method utilizes the Green-Kubo relation which gives the diffusion coefficient in terms of the velocity autocorrelation function. A second approach monitors the mean square displacement of the particle as a function of time and uses the well-known Einstein relation,

$$D = \lim_{t \to \infty} \frac{1}{6t} < |\mathbf{r}(t) - \mathbf{r}(0)|^2 >, \tag{2}$$

where $\mathbf{r}(t)$ is the coordinate of the particle at time t, to derive D.

The Einstein relation appears preferable to the calculation of the velocity correlation function approach.[11] We use the Einstein relation here. The simulation results obtained here and experimental values are given in Table III.

The values for D given in the table are obtained by linear least squares fit of the mean square displacement over the time interval from 1.0 to 2.0 ps. We are most interested in the qualitative differences among the ionic diffusion coefficients obtained, and we do not place heavy emphasis on the precise values. However, based on our experience, particularly with the longer simulations of Model 2, we believe that the values given are accurate to about

10%.

We first introduce the results obtained for the solvated electron, since they will be used as a reference point in the analysis of the other models studied here.

We analyze the dynamics of the electron semiclassically by monitoring the time dependence of the expectation value of the position of the center of mass. This is valid since the electron is well localized at all times.

The mean-square displacement of the electronic center of mass is displayed in Figure 2a, along with the mean-square displacement for the diffusion of all water molecules in the simulation cell. For the sake of comparison, we also show results for the classical bromide ion (Model 1; see Section IIIA). Figure 2b displays the short-time (non-diffusive) regime for the same species. Figure 3 shows the relative probability for center-of-mass displacements for each particle during time intervals of 20 (Fig.3a) and 200 (Fig.3b) femtoseconds. The results for the excess electron agree with those obtained by Schnitker and Rossky.[5]

As can be seen from Table III, the diffusion coefficient of bromide obtained here is in good agreement with the experimental value,[21] contrary to the result obtained from Schnitker and Rossky's calculations.[5] The individual values of D_{e^-} and of D_{Br^-} are each within about 20% of experiment. Further, the $\frac{D_{e^-}}{D_{Br^-}}$ ratio we obtain (1.6) is in reasonable agreement with the ratio obtained from experimental results (2.1).[21,22] We note that the value for D_{H_2O} is more than 50% too high (see Table III), as has been found for a

number of models.[9,23] The possible implications of this and of the apparent coincidence of the electron and solvent diffusion coefficients in the present calculation are discussed further below.

The much better agreement with experiment obtained here for the atomic ion appears to be a direct result of the introduction of the Ewald treatment of long range forces in place of the smooth truncation at a finite distance of about $8\mathring{A}$.[5] Corroborating results have appeared elsewhere,[5,20,23,24] although the large effect does not appear to have been emphasized by others. The enhancement in the diffusion coefficient due to the use of Ewald summation is about a factor of three. This separate aspect of the ion transport problem will be the subject of a separate report. Here, we use an Ewald treatment throughout, as noted earlier.

We now consider the results obtained for the model potentials introduced in Section III.

Figure 4 shows the ionic mean-square displacement and, Fig.5, the relative probability for center-of-mass displacement using Model 1 (Section IIIA). Each graph displays the results for the classical ion, for the corresponding adiabatic ion case, and for the solvent as well.

It is evident from the behavior exhibited by the solute that adiabaticity alone does *not* lead to an enhancement of a particle's diffusion rate, in contrast to what was previously suggested.[5–7] Comparing the ionic short-time behavior illustrated in Figures 4b and 5 with the electron results in Figures 2b and 3a, we can see that the instantaneous response of the ion does not

fully reproduce the characteristic motion exhibited by the excess electron, although the trend is correct.

The very short time behavior of the ion, reflected in Figure 4b, suggests that the steep repulsive ion-solvent interaction (see Fig.1) causes the ion to be repelled before being able to fully follow the changes in solvent configuration.

This speculation, in fact, led us to examine the other interaction potentials, with physically softer short-range ion-solvent repulsive components.

For Model 2, the ionic short-time behavior of the adiabatic case, displayed in Figure 6b, is in good agreement with the excess electron behavior. The probability distribution for displacement of the particles during a time span of 20 femtoseconds (Fig.7) exhibits behavior more closely analogous to the electron as well. For the ionic adiabatic dynamics, the distribution is shifted to larger distances and is asymmetric, unlike the sharp distribution observed for the classical ion. Nevertheless, from Figure 6a and Table III, it is evident that the softness of the repulsive part of the potential is not sufficient to fully explain the enhanced electronic diffusion rate.

It is also important to note that the classical calculations employing the softer potential characterizing Model 2 do *not* exhibit any significant enhancement in the diffusion rate or short time displacement over the normal ionic case. Further, we note that while Models 2 and 3 are characterized by somewhat weaker ion-solvent interactions than is Model 1 (see Fig.1; Table III). The substantial similarity in diffusion coefficients obtained with Model 1 and Model 2 indicates that the absolute strength of the interaction potential

is not a critical factor in this regard.

We now turn to further modification of the pseudoclassical model. As described above, the third and final model incorporates a distributed charge distribution for the ion which is, in principle, more realistic. In Model 3, we replace the point charge ion by a Gaussian charge distribution of constant width, and adjust the parameters corresponding to the short-ranged component in order to preserve a similar soft repulsive potential as well (see Section IIIC).

We can verify that the model used mimics the effect of the true distributed charge *a posteriori*. Fig.8 compares the actual average electrostatic solvent-solute interaction as a function of separation for the models of Br^-, e^-_{aq}, and the pseudoclassical Model 3. It is clear that Model 3 manifests results remarkably similar to the electron, and significantly different from those for the conventional ion.

Figures 9 and 10 show the results obtained with Model 3. We first note the fully classical(inertial) treatment of Model 3 yields only a small increase in D (Table III), amounting to only about 15% over the Lennard-Jones ion (Model 1). However, for the adiabatic dynamics of Model 3, not only does the short-time behavior of the ion closely mimic that of an electron (compare Fig.2b and 3 with Figures 9b and 10), but there is also a significant enhancement of the ionic diffusion rate when comparing the classical and adiabatic cases (compare Fig.2a and Fig. 9a; see Table III). The ionic diffusion is increased by a factor of about 1.5. The adiabatic Model 3 yields an increase over the

classical Lennard-Jones ion (Model 1) of 1.7, actually slightly greater than the factor of approximately 1.6 for the $\frac{D_{e^-}}{D_{Br^-}}$ ratio, from quantum simulations.

The probability distributions for the ionic displacements and solvent for a time span of 200 femtoseconds (Figure 10b) agree remarkably well with the probability distributions shown in Figure 3b, again indicating that there are no rapid translations("hops") of the solute over relatively large distances, and that this mechanism does not need to be invoked to substantially explain the ionic and/or electronic motions.

It is reasonable to attribute the additional enhancement of the diffusion coefficient for Model 3 over Model 2 to a decrease in rigidity of the solute-solvent complex. Such explanations have been introduced in discussing simple atomic ion diffusion,[24] and it is evident from Fig.8 that the electrostatic component of the energy is more slowly varying. Further, Fig.1 shows that in the penetrable model, the configurations with dipole aligned orientations are relatively considerably more stabilized. (Nevertheless, the structure of the *solution* remains dominated by bond oriented molecules, as will be shown below). Hence, we assign the principle difference in such rigidity here to the angular dependence of the interaction.

B Velocity autocorrelation functions

To obtain further insight into the microscopic dynamics of the species studied here, we have calculated for each case the velocity autocorrelation function, defined as

$$Z(t) = \frac{< \mathbf{v}(t) \cdot \mathbf{v}(0) >}{< |\mathbf{v}(0)|^2 >}, \tag{3}$$

where $\mathbf{v}(t)$ is the velocity of the particle at time t.

For the adiabatic calculations, including those for the electron itself, the effective solute velocities must be obtained indirectly. The implicit velocities are obtained using the central difference expression,

$$\mathbf{v}(t) = \frac{\mathbf{r}(t+1) - \mathbf{r}(t-1)}{2\Delta t}. \tag{4}$$

In Figure 11, we compare the velocity autocorrelation function of the classical bromide with the adiabatic velocity correlation function for the excess electron and for Model 3. The differences in appearance among the functions $Z(t)$ for the different models are relatively small, so that in the figure (Fig.11b) we show only one of the adiabatic pseudoclassical models.

The electron exhibits rapid velocity reversal, and a small high frequency modulation associated with the high-frequency solvent polarization fluctuations. These fluctuations are related to the rapid molecular librations in the hydrogen bonded solvent which also characterize the short-time dynamics of the excess electron (Figure 2b).

In contrast, the classical bromide ion shows no recoil and is remarkably Brownian in appearance. This picture is somewhat different from the oscillatory motions that have been reported[24] for the lighter and smaller ions F^- and Cl^-. These have been rationalized as the result of the ions "rattling" in

a relatively rigid solvent cage.[24] However, the trend with increasing ion mass is consistent, and one cannot rule out a contribution due to system size; the much earlier calculations employed a solvent system size of only 64 or 125 molecules, compared to the present 500 molecules.

The equilibrium average of v^2 equals $\frac{3k_BT}{m}$ by the principle of equipartition of energy, where m represents the mass. It is interesting to use this relationship to examine how the apparent effective mass varies with the interaction potential for the adiabatic cases.

For the electron we find (all values in amu) 0.8, while for Model 1 through 3 we find 5.0, 1.6, and 1.5, respectively. For Models 2 and 3 the apparent kinetic masses are close to that of the electron (and also that of the solvent proton), while for the Lennard-Jones ion it is substantially larger. We note that the fact that this effective, kinetic, mass corresponds to that of the proton does not imply that the ion is following the solvent *translationally*. The latter might also be inferred from the results for the mean squared displacement for Model 3 and e^-_{aq}, and this will be discussed further below. However, it is clear that for Model 2 the ionic diffusion is considerably slower than that of the solvent, or of the Model 3 ion, while the effective mass is comparable to Model 3, in accord with our comments above.

C Structure and energetics

The average electronic binding energy(-2.72 eV), and radius of gyration (2.14 Å) obtained here are in agreement with previous simulations of e^-_{aq}.[5,17]

Due to the fact that aspects of the electronic kinetic energy are incorporated into the model potentials of Models 2 and 3, a direct comparison of the absolute energetics of the pseudoclassical models to the quantum case is not possible. However, for completeness we include in Table III the average potential energies for all cases studied.

Of more interest are the structural features, which are directly comparable. This is done in Fig.12. The comparison is quantified further in Table IV.

Figure 12a shows the radial pair correlation functions between the electronic center of mass, and either oxygen or hydrogen nuclei of the solvent. The graphs exhibit the established bond oriented type of solvation, and the strongly broadened peaks, characteristic of the e^-_{aq} structure.[16,17]

The radial distribution functions of the solvated ion for the other models studied here are shown in Fig.12b-d. The only difference observed between the functions obtained for the classical, and the adiabatic cases is that the latter show somewhat more structure for the first layer peaks. This behavior is likely related to the fact that the solute-solvent potential energies are somewhat more positive for classical as compared to adiabatic dynamics (see Table III). For simplicity, we show only the pair correlation functions corresponding to the adiabatic calculations.

Figure 12b, corresponding to Model 1 shows radial correlation functions that are typical of a hydrated ion, with a sharply defined solvation layer.

For Model 2, the improvement in mimicking the structural features of e^-_{aq}

is striking (Fig. 12c). The correlation functions exhibit a much more diffuse nature, characteristic of the electronic solvation structure.

Figure 12d shows the results obtained for Model 3. The peaks are further broadened and the maxima and minima are decreased in height; the second ion-oxygen peak is slightly shifted outward (see Table IV). Overall, Model 3 is remarkably good at mimicking the structure exhibited by the solvated electron.

V CONCLUSION

Using a pseudoclassical technique that mimics the adiabatic dynamical response of a solvated electron, we have studied the diffusive behavior of bromide-like ions in water for different solute-solvent potential models. The dynamics incorporates an ion that responds instantaneously to the rearrangements of the solvent configuration, and lacks any classical inertial behavior. The results obtained were used as a tool to elucidate the origins of the transport behavior for a localized solvated electron.

We have shown that the enhancement of the electronic diffusion rate in the quantum simulations over the rate exhibited by classical ions can be attributed only partially to the adiabatic dynamics of the excess electron *per se*, although it is essential. We find that specific features of the solute-solvent interaction potential are also essential to the description of the mobility of the hydrated electron. These features include, first, the relatively weak forces that derive from the variation of the quantum kinetic energy with the spatial

confinement of the excess electron. The kinetic energy effect can be modeled by a soft repulsive solute-solvent interaction and it is manifest primarily in the non-diffusive electronic motion on time scales of 0.2 ps and less. Second, the electrostatic interaction of the electron and solvent is much more realistically described when one allows partial penetration of the excess electronic distribution by molecules of the first hydration shell. This second feature predominantly contributes to the enhancement of the (longer time scale) electronic diffusion rate. We have attributed this latter effect to the orientation dependence of electron-solvent interaction.

In addition to dynamical properties, the model that best reproduces the electron mobility observed from quantum mechanical calculations also mimics the simulated solvated electron solvation structure very well.

Before completing the discussion, a possible alternative view of the present work should be noted. As pointed out earlier, although the electronic and ionic diffusion coefficients are mimicked well by the present calculations, the electron and solvent are observed to diffuse at the same rate; experimentally, the electron diffusion coefficient is about twice that of water. Based on this coincidence of electron and solvent diffusion rates, one possible interpretation of the simulated data discussed here is that the electron is translationally following the solvent in *both* the pseudoclassical and quantum simulations. A tendency toward this view can be readily amplified by the physical picture associated with adiabatic electronic motion.

Such a conclusion would have profound implications for this, and all re-

lated, work. Implicitly, the electronic diffusion rate observed in the present simulations would then be only half what it "should" be in SPC model water for a realistic electronic solute. Correspondingly, one would be forced to conclude that the quantum simulations of electrons in water are lacking in some fundamental way. On the basis of the data presented in the present paper, we cannot categorically rule out this possibility. However, we believe that this observation of similar diffusion coefficients is basically accidental, a result of limitations of the SPC model.

We note first that the coincidence of two diffusion coefficients is not strong evidence for a physical picture. The diffusion constants of water and Bromide are nearly the same experimentally (see Table III), and such a physical picture would not be invoked in that case. Further, one would then need to ask why the other adiabatic ion models do *not* follow the solvent.

In addition, we note that such processes as hopping are not restricted by the methods we or others[6] employ in the quantum simulation, except for the restriction to electronically adiabatic dynamics. Non-adiabatic contributions are not plausible for this case, where the energy gap to excited states is always large.[16] Hence, the missing physical effect that would be required for this alternative interpretation is not self-evident. Nevertheless, it remains for further simulations with other water models to establish an unequivocal conclusion with respect to this issue.

Finally, the approach and results presented here suggest several further investigations. These include the use of the present model to elucidate the

apparently unusual thermodynamics of e^-_{aq},[25] and the temperature dependence of diffusion rates.[22] Although the latter phenomenon may depend on the variation of the pseudoclassical model parameters with temperature, it is reasonable to anticipate that such variation would not be a leading order effect. In addition, similar methods could, in principle, be applied to the study of electronic diffusion in simple alcohols, in order to test hypotheses[22] for contrasting behavior in that case. Although here we have used the quantum simulation as a source for the parameters of the pseudoclassical model, an analysis of experimental spectral data would have yielded very similar parameters,[26] and that approach may allow an *a priori* generalization to other systems.

Acknowledgment

The work reported here has been supported by a grant from the Office of Naval Research. Further support has been provided by a grant from Robert A. Welch Foundation (F-0761). The computational support of the Center for High Performance Computing of the University of Texas System is also gratefully acknowledged.

References

[1] Hart, E. J.; Boag, J. W. *J.Am.Chem.Soc.* **1962**, *84*, 4090.

[2] (a) Schmidt, W. F. In *Electron-Solvent and Anion-Solvent Interactions*; Kevan, L.; Webster, B. C., Eds.; Elsevier: Amsterdam, 1976. (b) Feng, D. F.; Kevan, L., *ibid.*

[3] McHale, J.; Simons,J. *J.Chem.Phys.* **1978**, *68*, 1695.

[4] Hameka, H. F.; Robinson, G. W.; Marsden, C. J. *J.Phys.Chem.* **1987**, *91*, 3150.

[5] Schnitker, J.; Rossky, P. J. *J.Phys.Chem.* **1989**, *93*, 6965.

[6] Barnett, R. N.; Landman, U.; Nitzan, A. *J.Chem.Phys.* **1990**, *93*, 8187.

[7] (a) Sprik, M.; Klein, M. L. *J.Chem.Phys.* **1988**, *89*, 1592. (b) *ibid.* **1989**, *91*, 5665.

[8] Wolynes, P. G. *Annu.Rev.Phys.Chem.* **1980**, *31*, 345.

[9] Berendsen, H. J. C.; Postma, J. P. M.; Van Gunsteren, W. F.; Hermans, J. In *Intermolecular Forces*; Pullman, B., Ed.; Reidel: Dordrecht, 1981.

[10] Ryckaert, J-P.; Ciccotti, G.; Berendsen, H. J. C. *J.Comput.Phys.* **1977**, *23*, 327.

[11] Allen, M. P.; Tildsley, D. In *Computer Simulation of Liquids*; Clarendon: Oxford, 1987.

[12] Press, W. H.; Flannery, B. P.; Teukolsky, S. A.; Vetterling, W. T. In *Numerical Recipes*; Cambridge University Press: Cambridge, 1990.

[13] (a) Forsythe, G. E.; Malcom, M. A.; Moler, C. B. In *Computer Methods for Mathematical Computations*; Prentice Hall: Englewood Cliffs, NJ, 1977. (b) Jacobs, D. A. H. In *The State of the Art in Numerical Analysis*; Academic Press: London, 1977. (c) Polak, E. In *Computational Methods in Optimization*; Academic Press: New York, 1971.

[14] Schnitker, J.; Rossky, P. J.; Kenney-Wallace, G. A. *J.Chem.Phys.* **1986**, *85*, 2986.

[15] (a) Schnitker, J.; Rossky, P. J. *J.Chem.Phys.* **1987**, *86*, 3462. (b) Webster, F. A.; Rossky, P. J.; Friesner, R. A. *Computer Physics Comm.* **1991**, *63*, 494.

[16] Rossky, P. J.; Schnitker, J. *J.Phys.Chem.* **1988**, *92*, 4277.

[17] Schnitker, J.; Rossky, P. J. *J.Chem.Phys.* **1987**, *86*, 3471.

[18] Palinkas, G.; Riede, W. O.; Heinzinger, K. Z. *Naturforsch.* **1977**, *32A*, 1137.

[19] Schnitker, J.; Motakabbir, K.; Rossky, P. J.; Friesner, R. A. *Phys.Rev.Lett.* **1988**, *60*, 456.

[20] (a) Wilson, M. A.; Pohorille, A.; Pratt, L. R. *J.Chem.Phys.* **1985**, *83*, 5832. (b) Berkowitz, M.; Wan, W. *ibid.* **1987**, *86*, 376. (c) Reddy, M. R.; Berkowitz, M. *ibid.* **1988**, *88*, 7104.

[21] Robinson, R. A.; Stokes, R. H. In *Electrolyte Solutions*; Butterworths: London, 1959.

[22] Schmidt, K. H.; Han, P.; Bartels, D. M. *J.Phys.Chem.* **1992**, *96*, 199.

[23] Sprik, M.; Klein, M. L.; Watanabe, K. *J.Phys.Chem.* **1990**, *94*, 6483.

[24] Impey, R. W.; Madden, P. A.; McDonald, I. R. *J.Phys.Chem.* **1983**, *87*, 5071.

[25] Han, P.; Bartels, D. M. *J.Phys.Chem.* **1991**, *95*, 5367.

[26] Tuttle, Jr., T. R.; Golden, S. *J.Phys.Chem.* **1991**, *95*, 5725.

[27] Mills, R. *J.Phys.Chem.* **1973**, *77*, 685.

Table I: Time intervals of simulations in picoseconds

Model	Br^-/H_2O 1	2	3	e^-_{aq}
Classical	100	60	40	-
Adiabatic	40	100	40	42

Table II: Parameters corresponding to the non-electrostatic component of the interaction potential functions.

Model	σ ($\AA$)	ϵ (kJ/mol)	A (kJ/mol)	B ($\AA^{-2}$)	C	α ($\AA^{-1}$)	D (kJ/mol)	β ($\AA^{-2}$)
1	4.16	0.214987	-	-	-	-	-	-
2	-	-	957.69	0.921	0.005	2.733	20000.0	1.513
3	-	-	957.69	3.420	0.01	2.733	-	-

Table III: Solute and solvent self-diffusion coefficients and average potential energies.

Model		D ($10^{-5} cm^2/sec$) classical	D ($10^{-5} cm^2/sec$) adiabatic	U (kJ/mol) classical	U (kJ/mol) adiabatic
1	H_2O	-	4.1	-41.2	-41.1
	Br^-	2.5	2.9	-604.0	-612.0
2	H_2O	-	4.0	-41.3	-41.3
	Br^-	2.7	3.0	-512.3	-515.4
3	H_2O	-	4.0	-41.4	-41.3
	Br^-	2.9	4.3	-505.7	-518.0
QMD	H_2O	-	4.1	-	-41.1
	e^-	-	4.0	-	-508.6
Experiment	e^-	-	5.0[a]	-	-
	Br^-	2.1[b]	-	-	-
	H_2O	2.3[c]	-	-	-

[a]Ref.22.
[b]Ref.21.
[c]Ref.27.

Table IV: Properties of peaks in radial pair correlation functions between solutes and oxygen (upper rows) or hydrogen (lower rows) nuclei for adiabatic cases.

	1st Maximum		1st Minimum		2nd Maximum	
Model	Position ($\AA$)	Height	Position ($\AA$)	Height	Position ($\AA$)	Height
1	3.3	4.0	4.0	0.47	5.0	1.2
2	3.3	1.8	4.1	0.56	5.0	1.3
3	3.3	1.7	3.9	0.70	4.8	1.2
e^-_{aq}	3.3	1.4	3.9	0.91	4.5	1.2
1	2.3	3.3	3.2	0.25	-	-
2	2.3	1.6	3.1	0.33	-	-
3	2.2	1.6	3.0	0.48	-	-
e^-_{aq}	2.3	1.2	3.0	0.64	-	-

Figure Captions

FIG. 1. Solute-solvent pair potential as a function of the bromide-oxygen distance. Model 1 (solid line), Model 2 (dashed line), Model 3 (dotted line). Horizontal and vertical axes in units of $\mathring{A}$ and kcal mol^{-1}, respectively. (a) ion collinear with the OH bond direction; (b) ion collinear with the HOH angle bisector.

FIG. 2. Mean-square displacement (msd) of centers of mass as a function of time for excess electron (dashed line) and water (solid line), from QMD simulation, and corresponding results for bromide ion (dot-dashed line) from classical molecular dynamics simulation using Model 1. Vertical axis in $\mathring{A}^2$, time in ps. (b) Shows the short-time dynamics on an expanded scale.

FIG. 3. Relative probability for center-of-mass displacements for solutes and solvent. (a) Elapsed time $\Delta t = 20$ fs. Excess electron (dashed line), water (solid line), classical bromide, Model 1 (dot-dashed line); (b) $\Delta t = 200$ fs. Excess electron (dashed line), water (solid line).

FIG. 4. Mean-square displacement (msd) of centers of mass as a function of time using Model 1. Adiabatic bromide ion (dashed line), water (solid line), and classical bromide ion (dot-dashed line). Vertical axis in $\mathring{A}^2$, time in ps. (b) Shows the short-time dynamics on an expanded scale.

FIG. 5. Relative probability for center-of-mass displacements for solutes

and solvent using Model 1, for a time interval of 20 fs. Adiabatic bromide (dashed line), water (solid line), and classical bromide ion (dot-dashed line).

FIG. 6. Mean-square displacement (msd) of centers of mass as a function of time using Model 2. Otherwise as in Fig. 4.

FIG. 7. Relative probability for center-of-mass displacements for solutes and solvent using Model 2. Otherwise as in Fig. 5.

FIG. 8. Average Coulombic interaction energy between a solvent molecule and the ionic solute as a function of the separation of the solvent oxygen atom and the ionic center of mass. Classical bromide, Model 1 (solid line); excess electron (dotted line); Gaussian charge model, Model 3 (dashed line). For Models 1 and 3, the results shown are from the adiabatic simulations. Horizontal and vertical axes in units of Å and kcal mol^{-1}, respectively.

FIG. 9. Mean-square displacement (msd) of centers of mass as a function of time using Model 3. Otherwise as in Fig. 4.

FIG. 10. Relative probability for center-of-mass displacements for solutes and solvent using Model 1. (a) Elapsed time $\Delta t = 20$ fs. Adiabatic bromide (dashed line), water (solid line), classical bromide ion (dot-dashed line); (b) $\Delta t = 200$ fs. Adiabatic bromide (dashed line) and water (solid line).

FIG. 11. Velocity autocorrelation function for the ionic center of mass. (a) Electron (dashed line); classical bromide ion (solid line), Model 1; (b) adiabatic bromide ion (dashed line), classical bromide, Model 3 (solid line).

FIG. 12. Solute-solvent pair correlation functions between solute center of mass and either solvent oxygen (solid line) or hydrogen (dotted line) from adiabatic simulations. (a) electron; (b) Model 1; (c) Model 2; (d) Model 3.

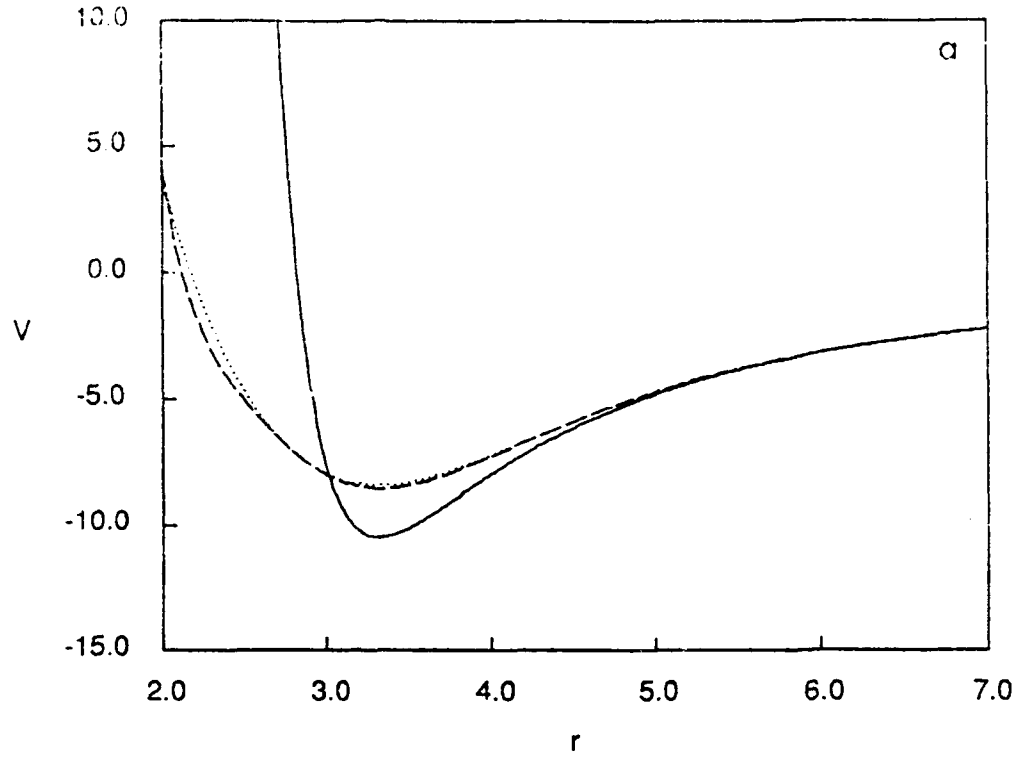
a
10.0
5.0
0.0
-5.0
-10.0
-15.0
V
2.0
3.0
4.0
5.0
6.0
7.0
r

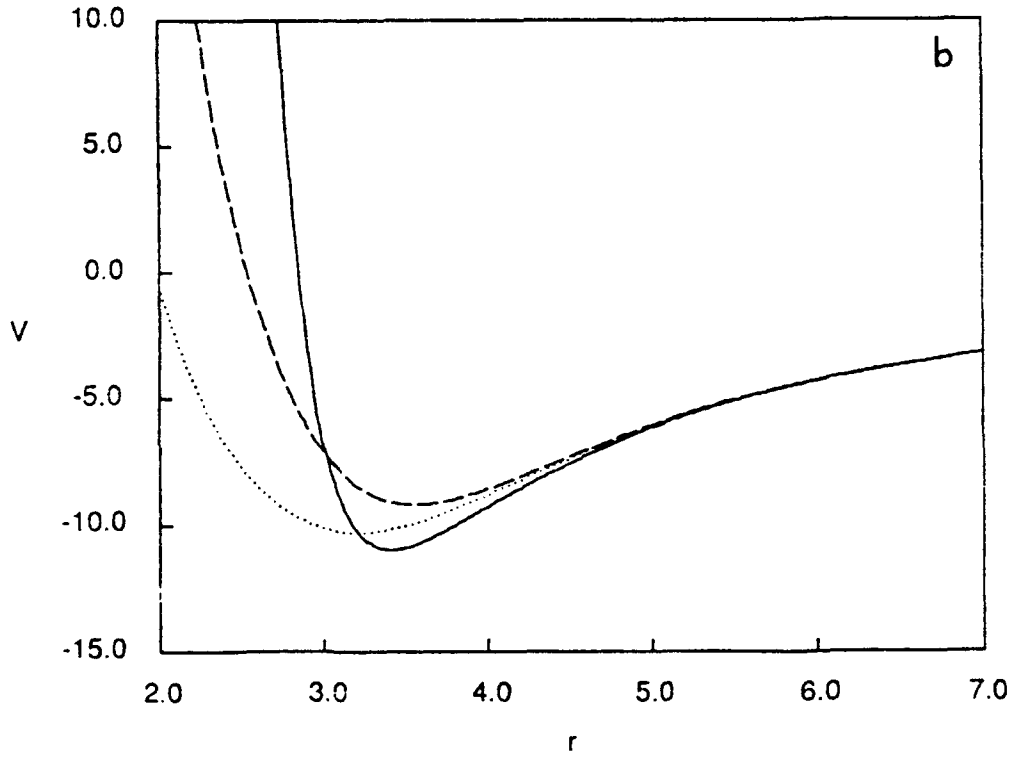
b
10.0
5.0
0.0
-5.0
-10.0
-15.0
V
2.0
3.0
4.0
5.0
6.0
7.0
r

Fig. 1

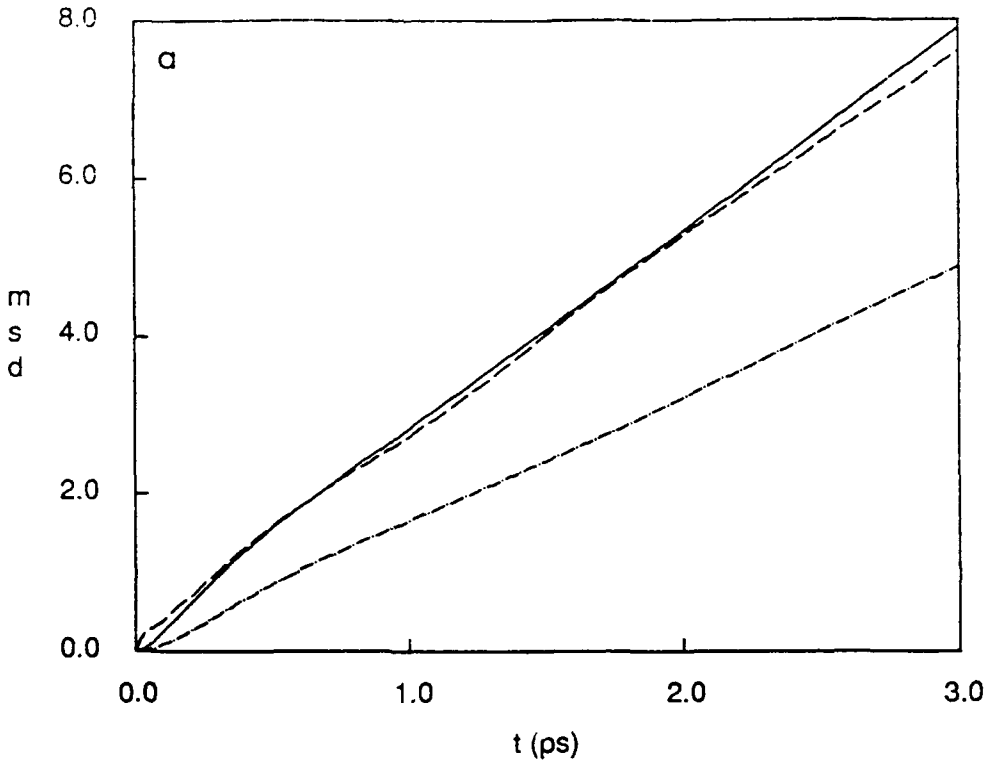

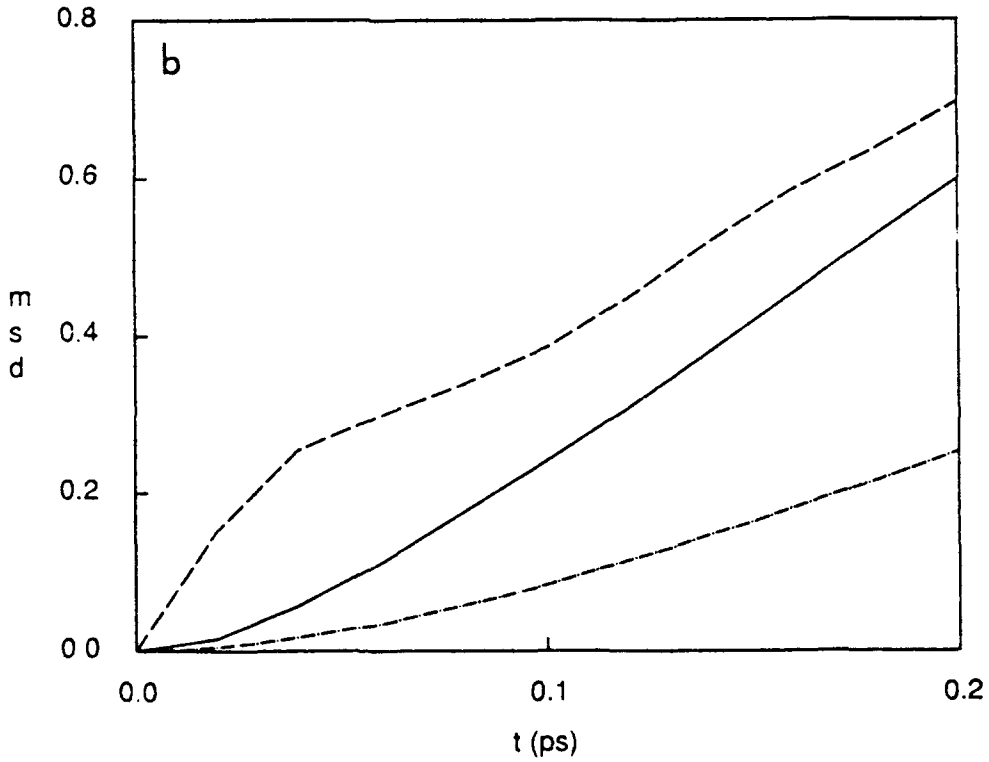

Fig. 2

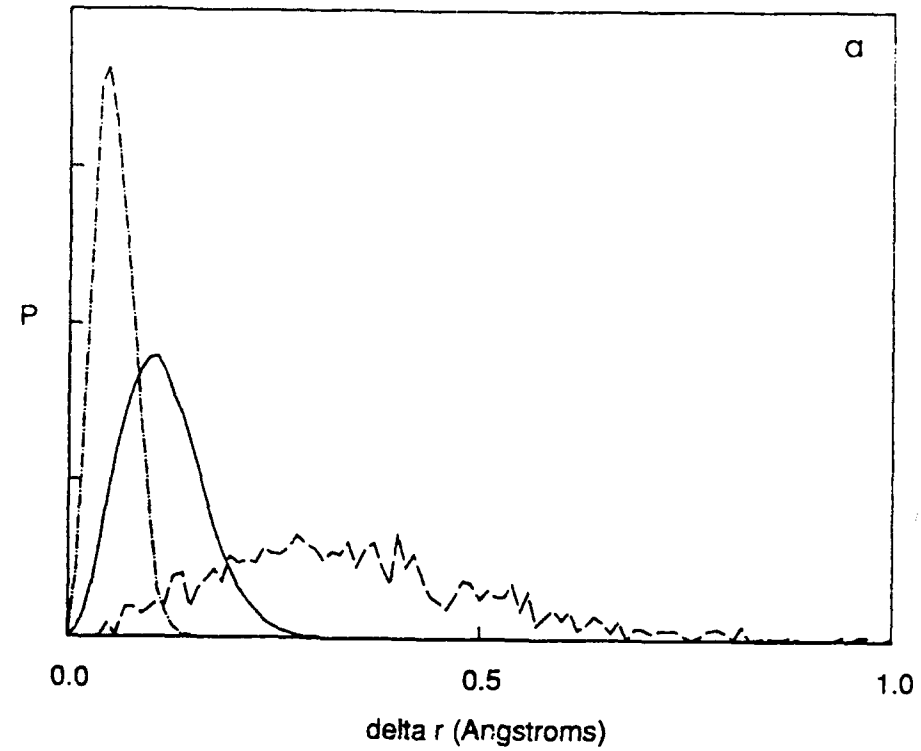
a
P
0.0
0.5
1.0
delta r (Angstroms)

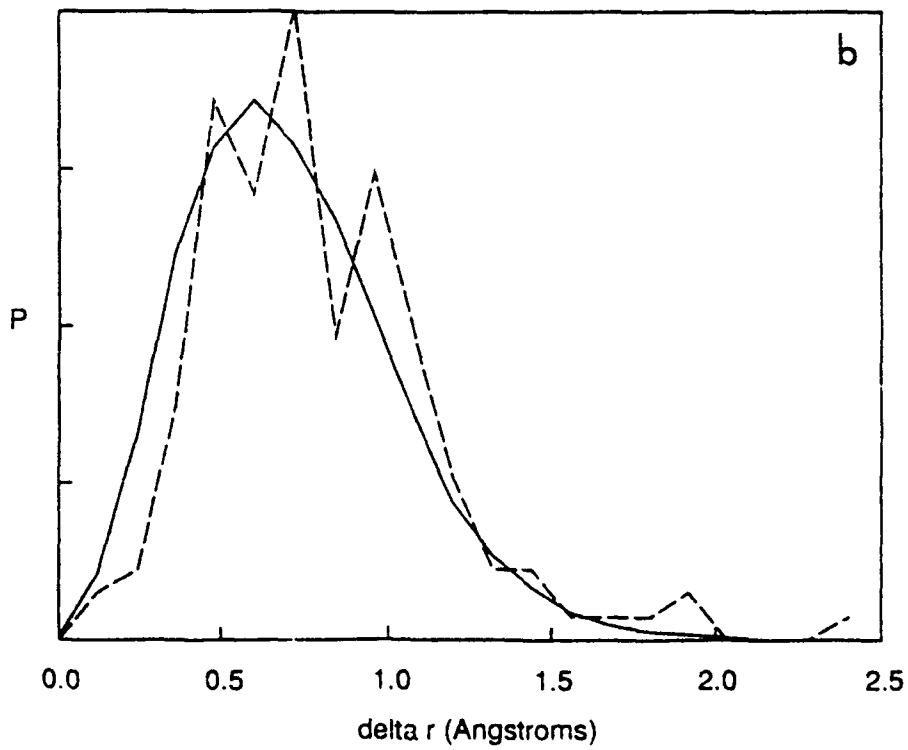
b
P
0.0
0.5
1.0
1.5
2.0
2.5
delta r (Angstroms)

Fig.3

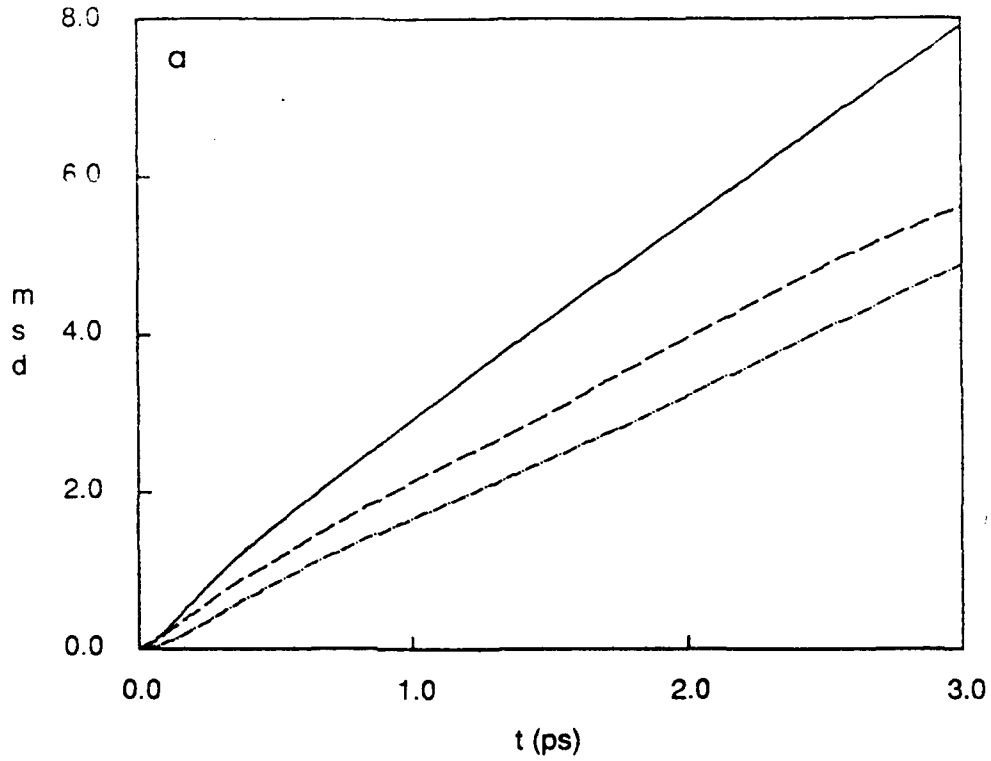

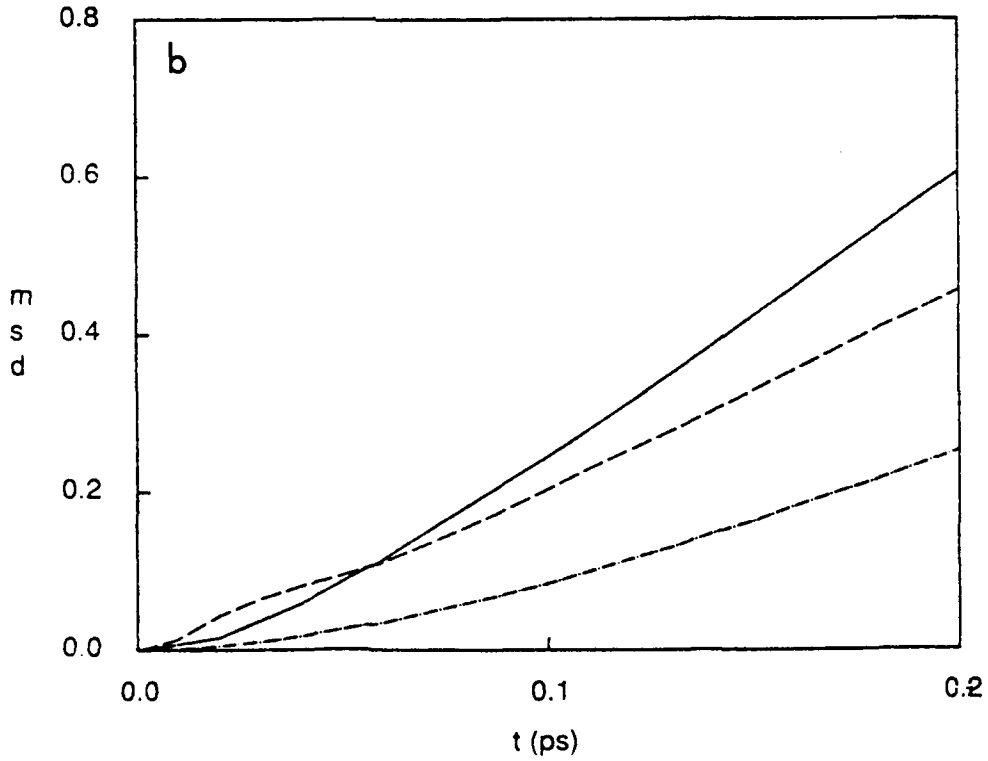

Fig. 4

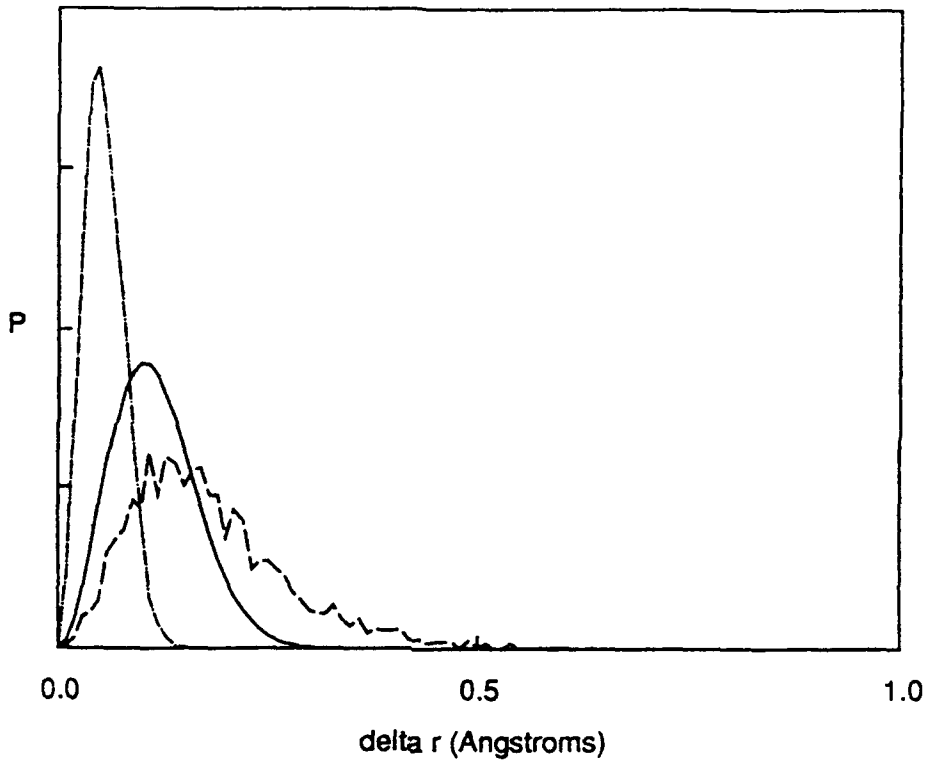

Fig. 5

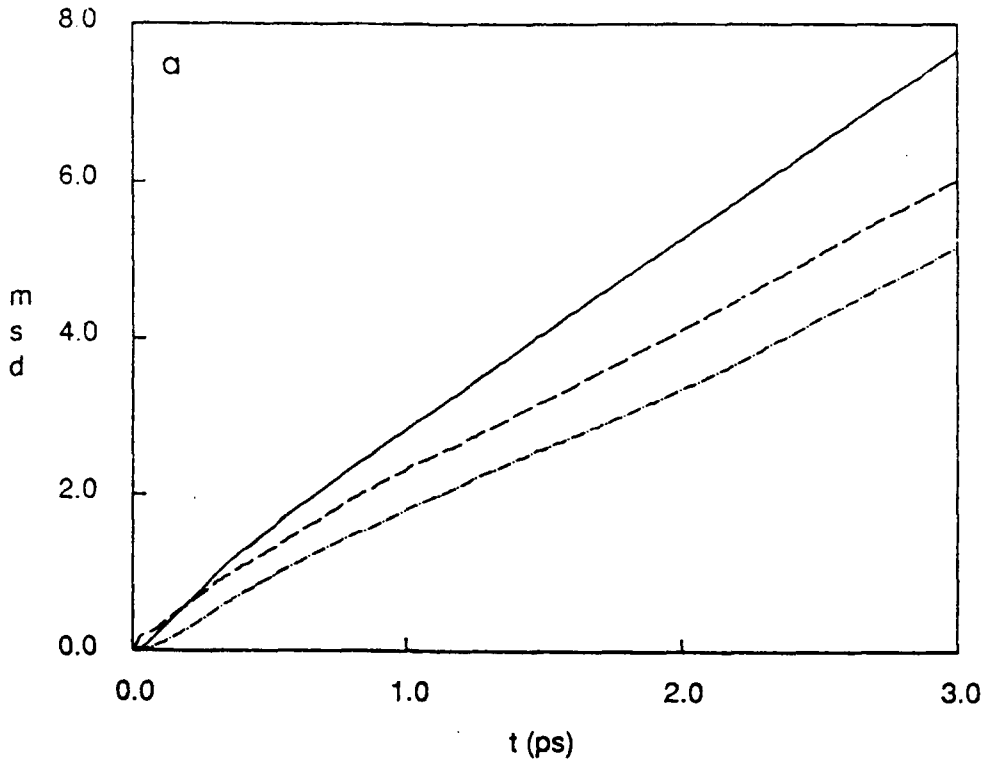

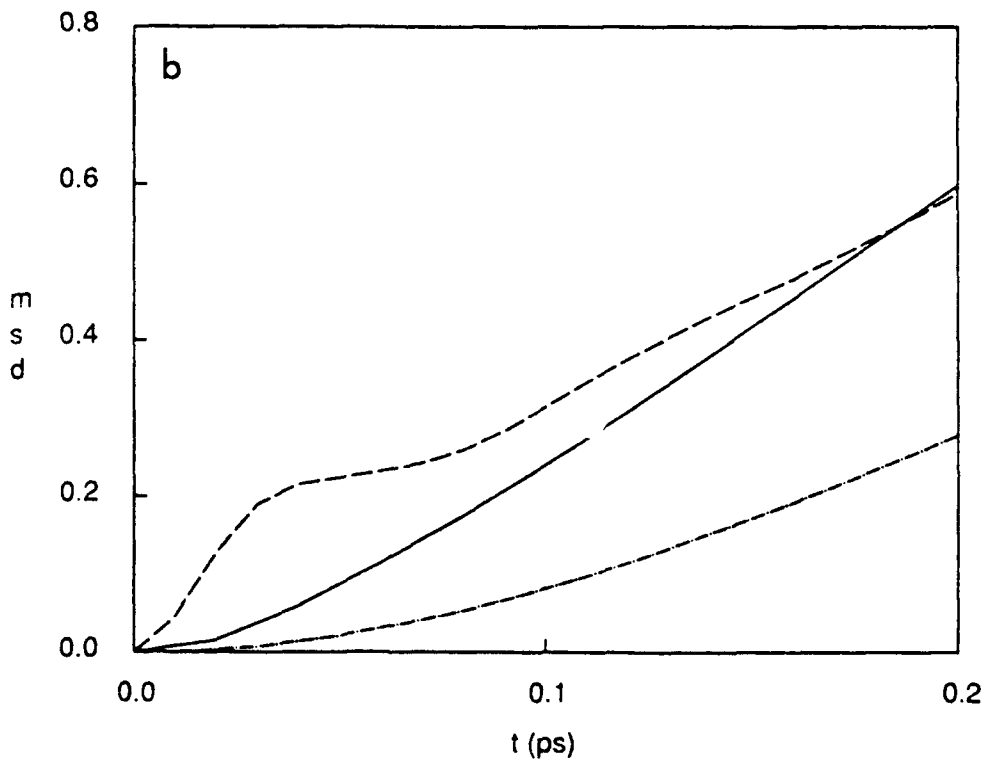

Fig. 6

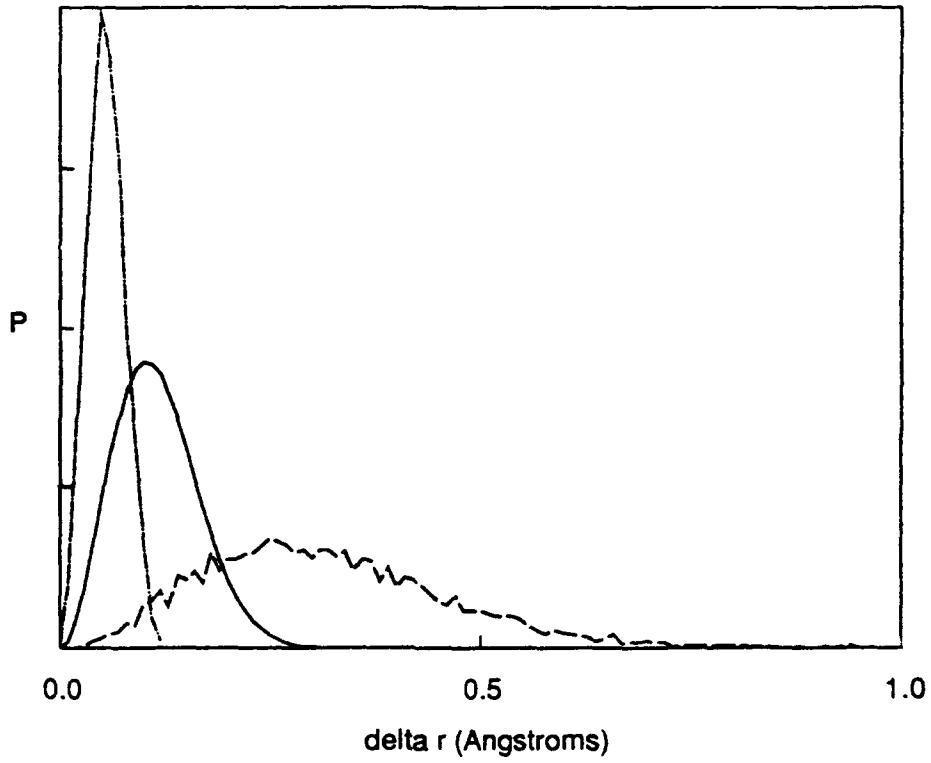

Fig. 7

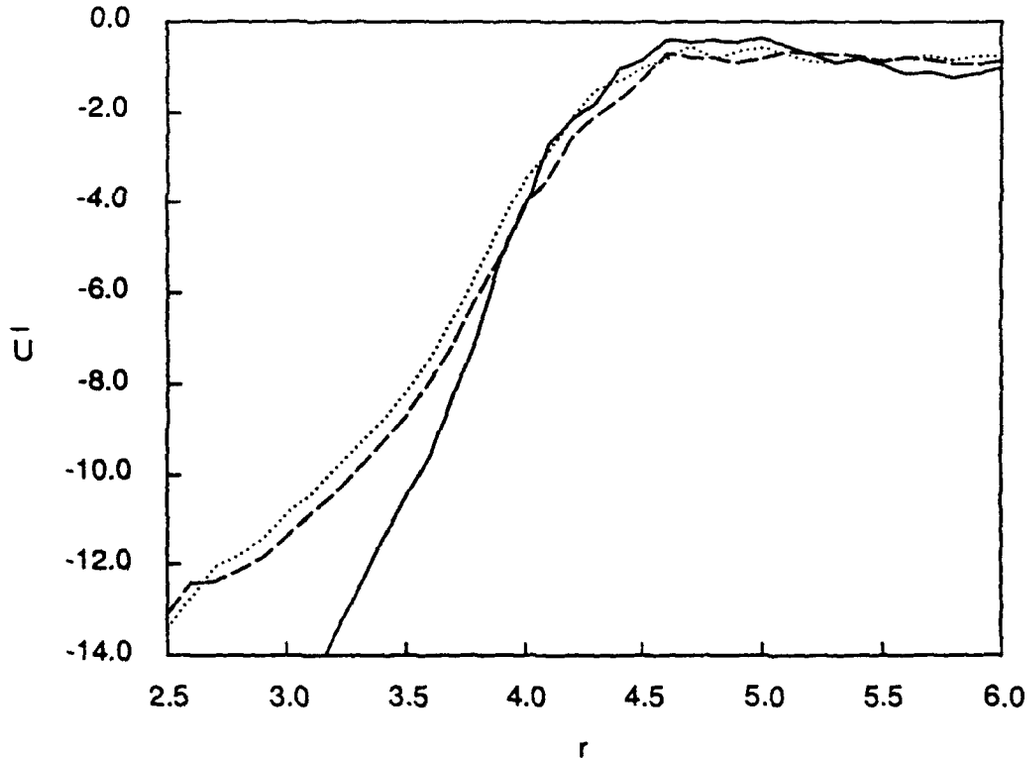

Fig. 8

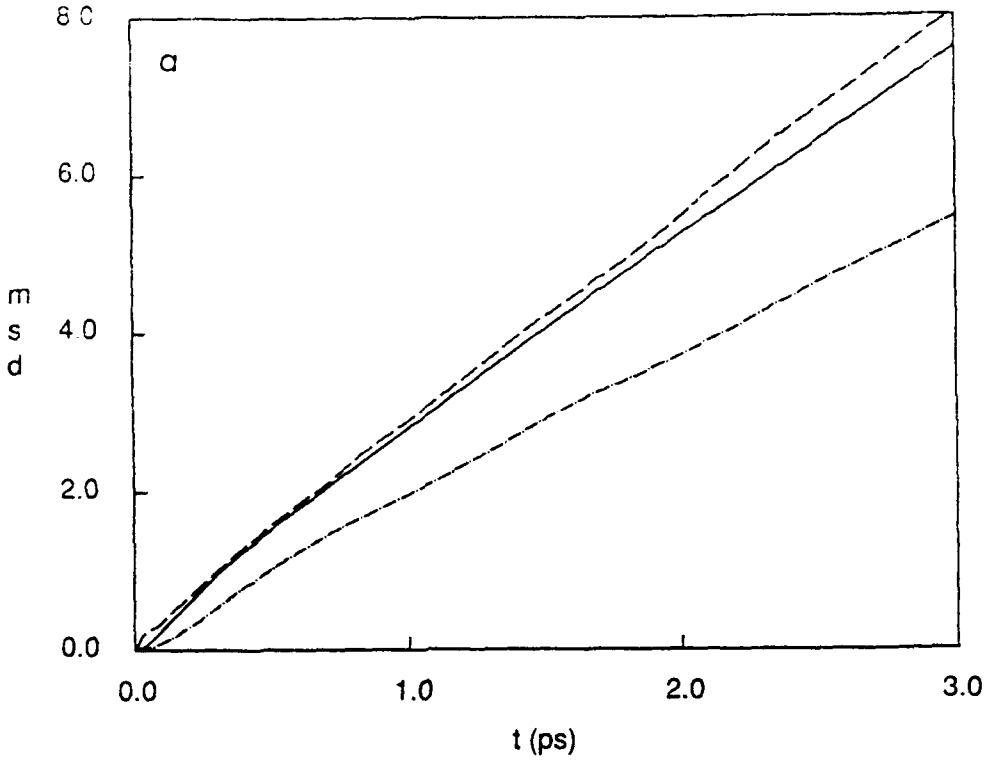

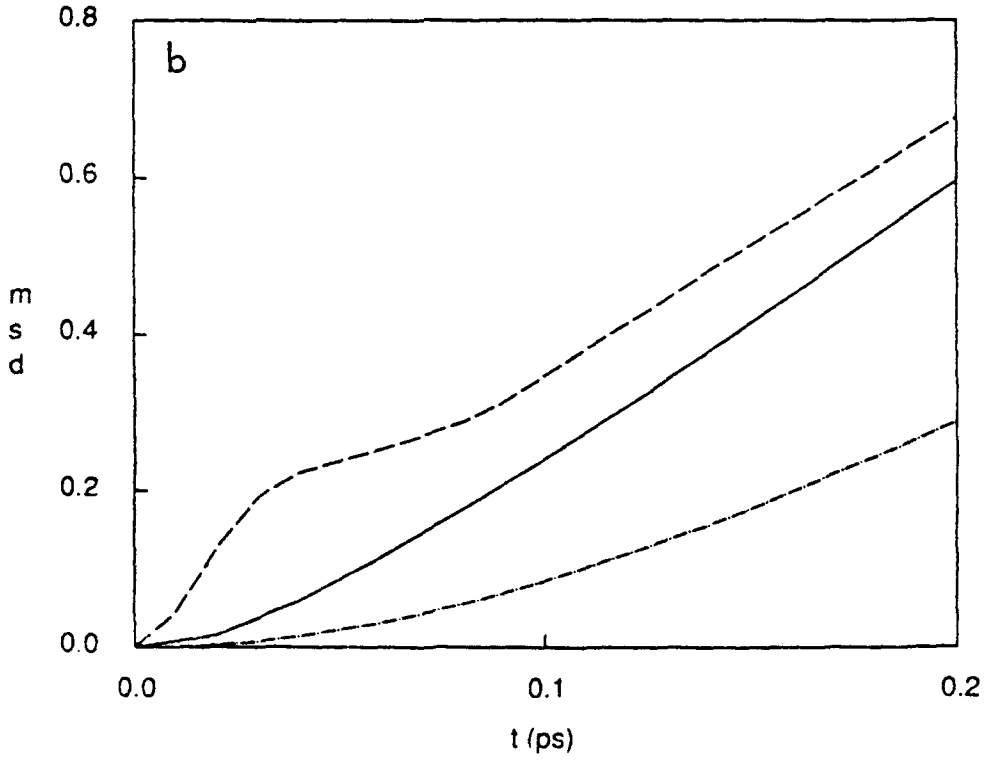

Fig. 9

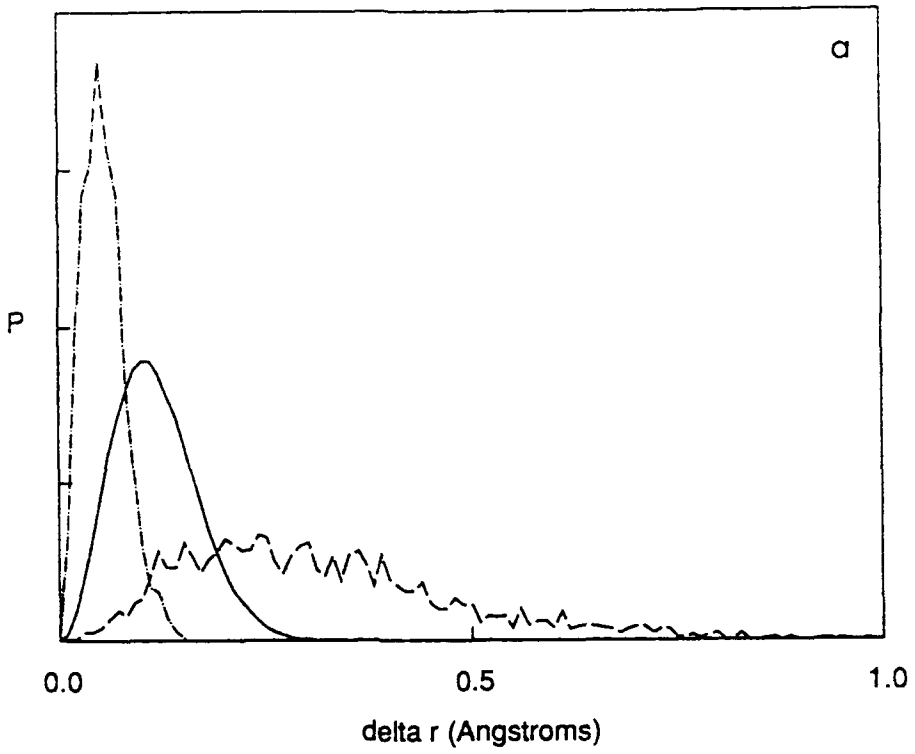
a
P
0.0
0.5
1.0
delta r (Angstroms)

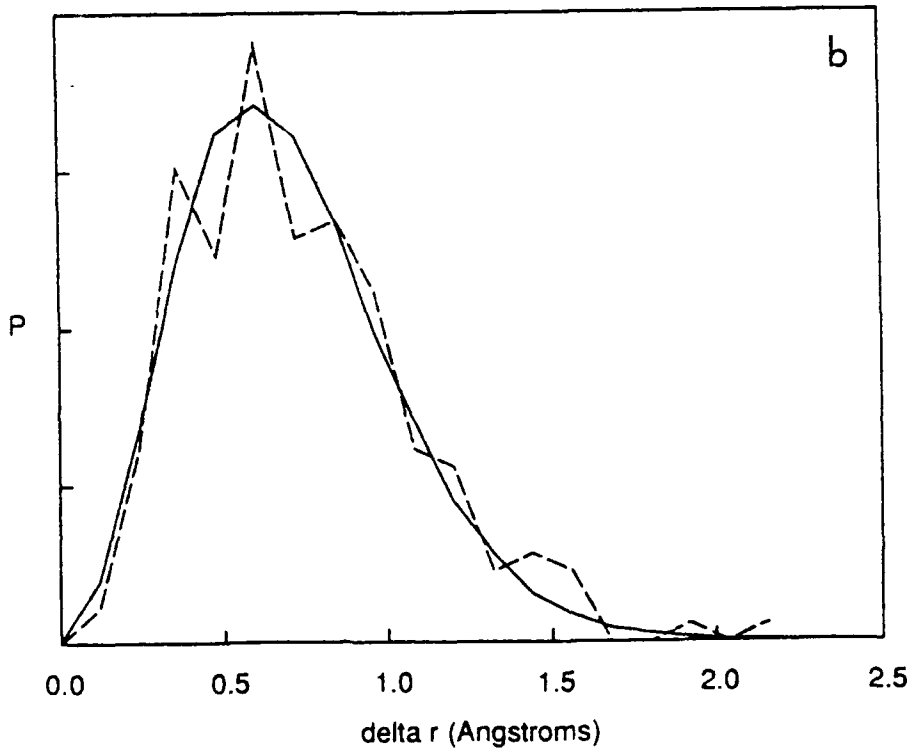
b
P
0.0
0.5
1.0
1.5
2.0
2.5
delta r (Angstroms)

Fig. 10

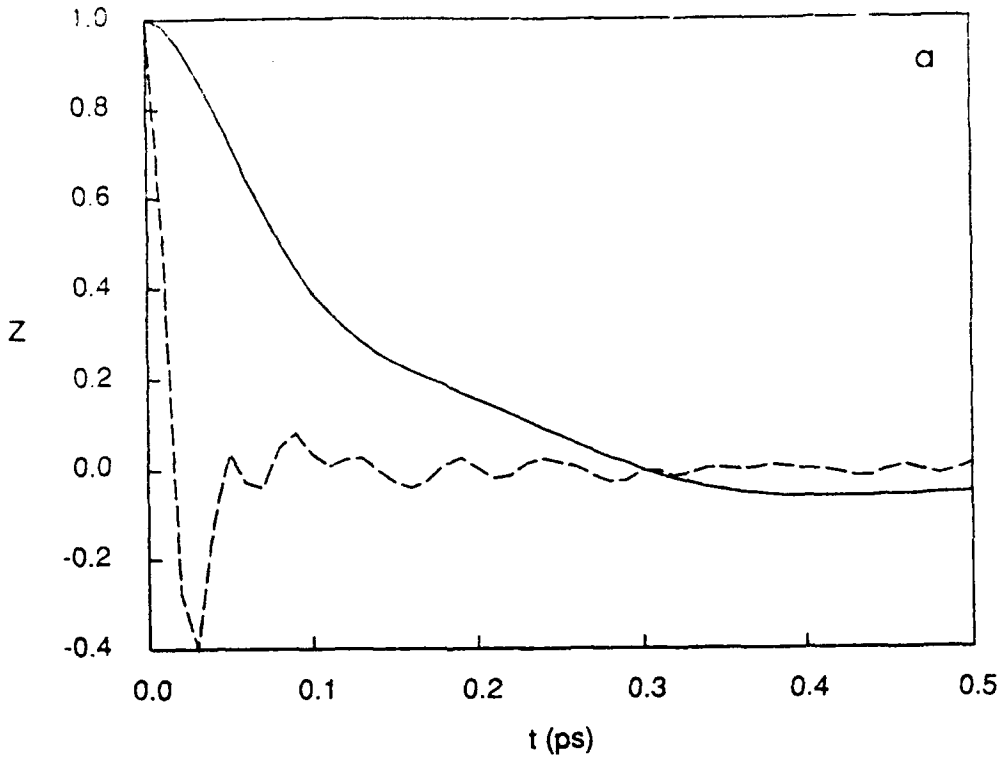
a
1.0
0.8
0.6
0.4
0.2
0.0
-0.2
-0.4
Z
0.0
0.1
0.2
0.3
0.4
0.5
t (ps)

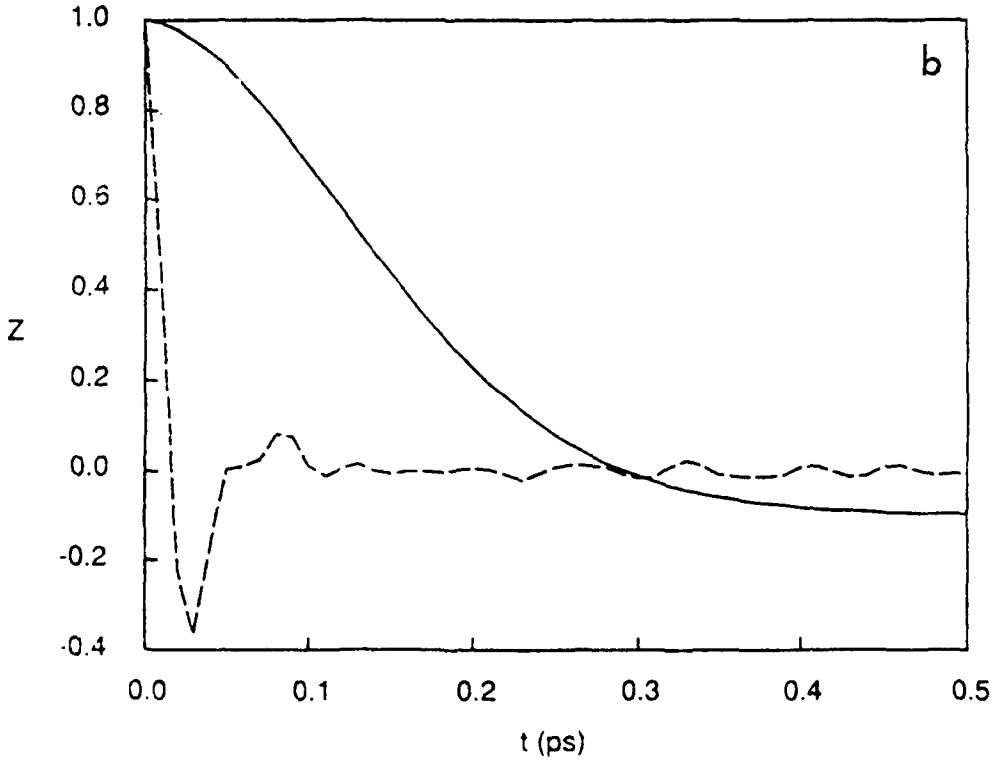
b
1.0
0.8
0.6
0.4
0.2
0.0
-0.2
-0.4
Z
0.0
0.1
0.2
0.3
0.4
0.5
t (ps)

Fig. 11

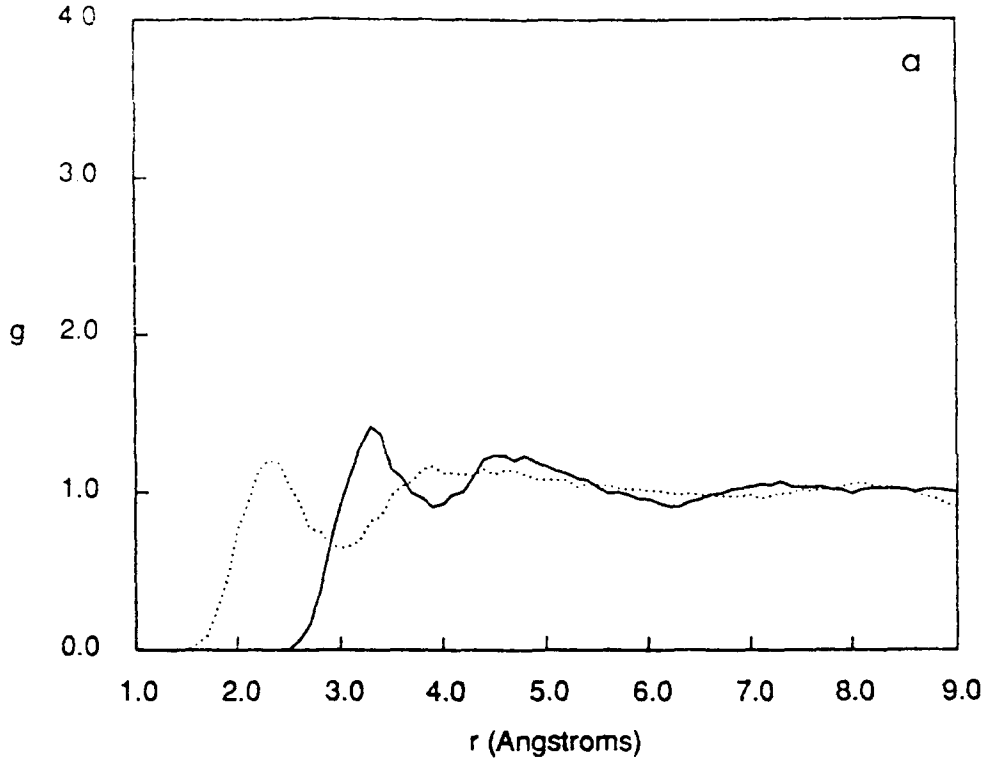
a
g
4.0
3.0
2.0
1.0
0.0
1.0
2.0
3.0
4.0
5.0
6.0
7.0
8.0
9.0
r (Angstroms)

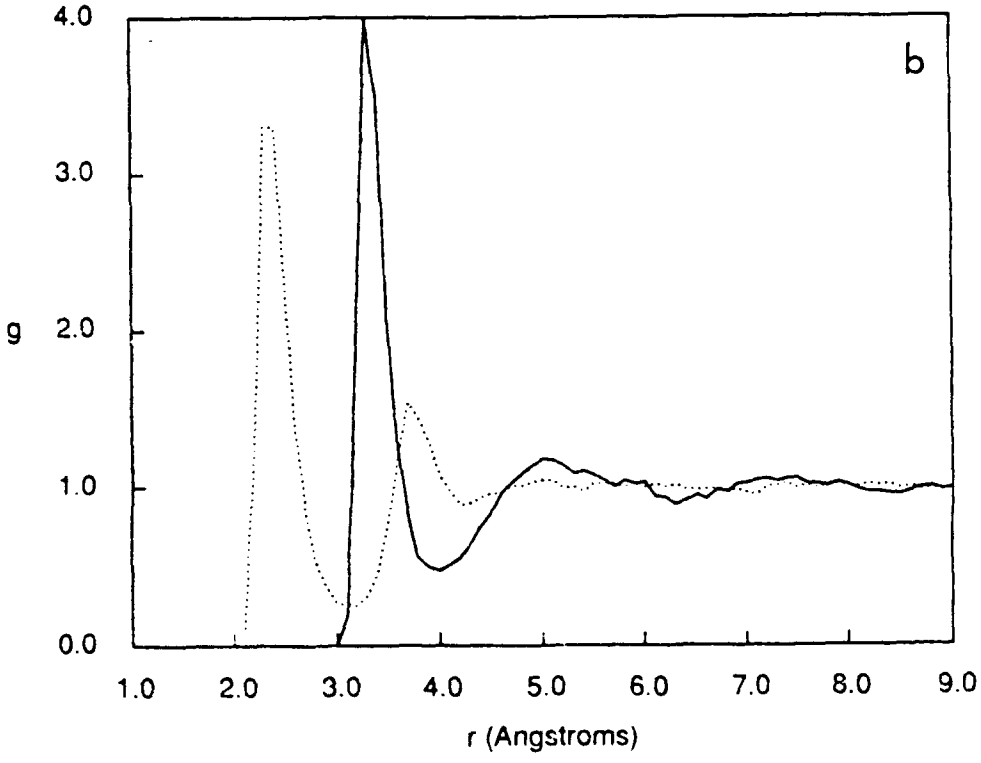
b
g
4.0
3.0
2.0
1.0
0.0
1.0
2.0
3.0
4.0
5.0
6.0
7.0
8.0
9.0
r (Angstroms)

Fig. 12a,b

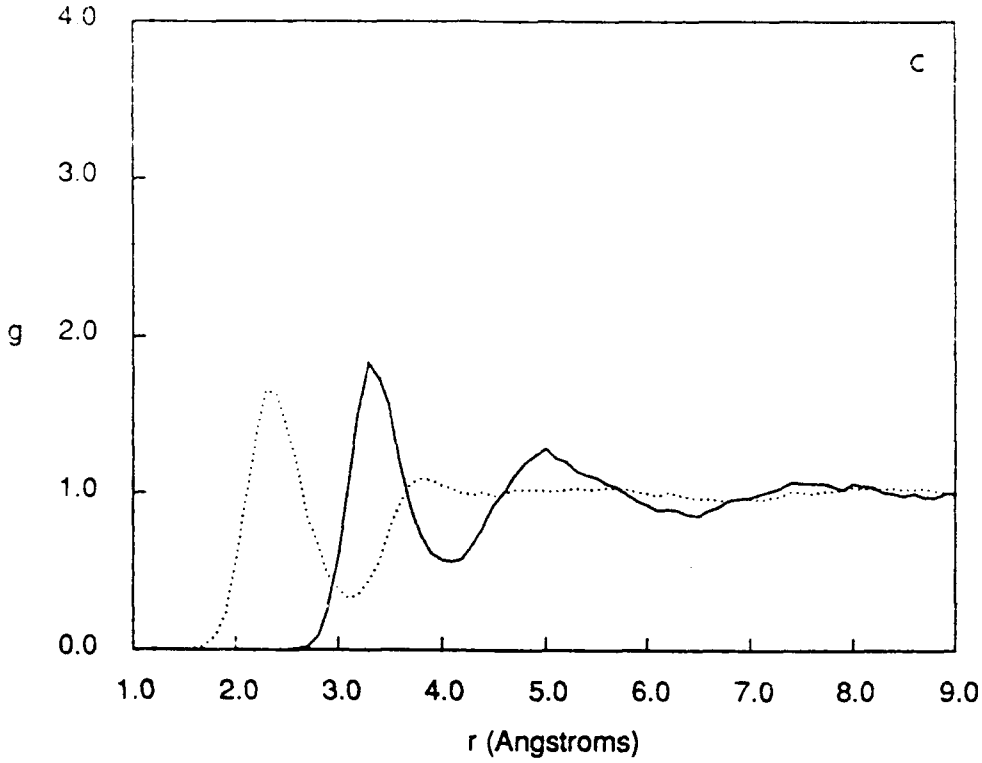
c
g
4.0
3.0
2.0
1.0
0.0
1.0
2.0
3.0
4.0
5.0
6.0
7.0
8.0
9.0
r (Angstroms)

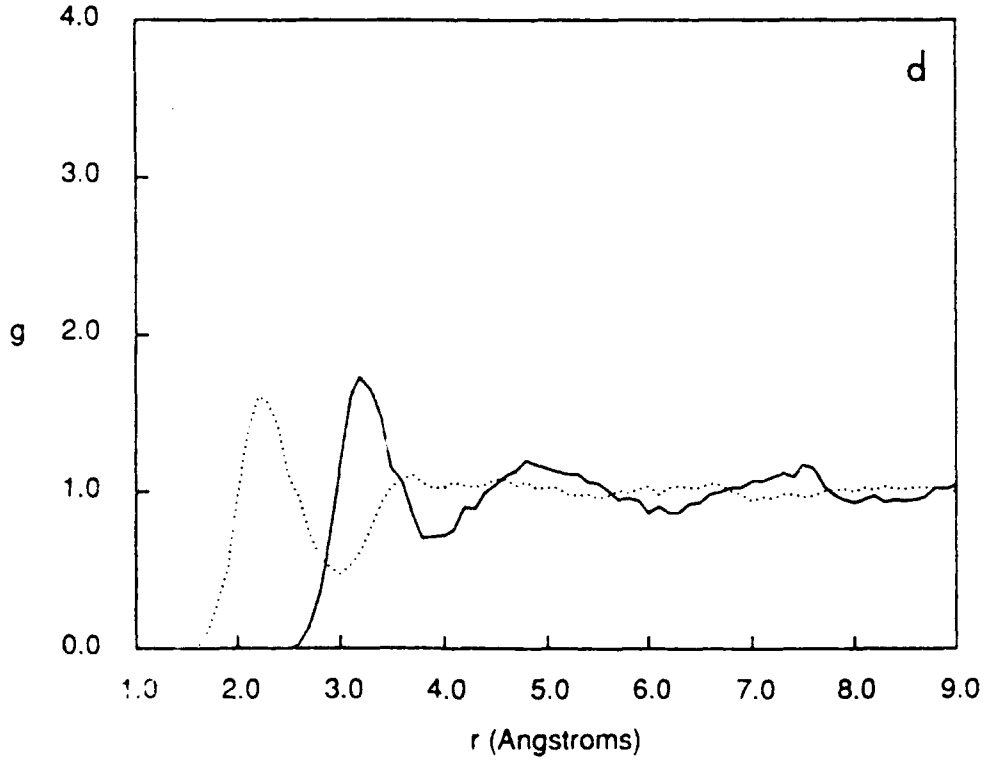
d
g
4.0
3.0
2.0
1.0
0.0
1.0
2.0
3.0
4.0
5.0
6.0
7.0
8.0
9.0
r (Angstroms)

Fig. 12 c,d

TECHNICAL REPORT DISTRIBUTION LIST - GENERAL

Office of Naval Research (2)*
Chemistry Division, Code 1113
800 North Quincy Street
Arlington, Virginia 22217-5000

Dr. James S. Murday (1)
Chemistry Division, Code 6100
Naval Research Laboratory
Washington, D.C. 20375-5000

Dr. Robert Green, Director (1)
Chemistry Division, Code 385
Naval Air Weapons Center
Weapons Division
China Lake, CA 93555-6001

Dr. Elek Lindner (1)
Naval Command, Control and Ocean
Surveillance Center
RDT&E Division
San Diego, CA 92152-5000

Dr. Bernard E. Douda (1)
Crane Division
Naval Surface Warfare Center
Crane, Indiana 47522-5000

Dr. Richard W. Drisko (1)
Naval Civil Engineering
Laboratory
Code L52
Port Hueneme, CA 93043

Dr. Harold H. Singerman (1)
Naval Surface Warfare Center
Carderock Division Detachment
Annapolis, MD 21402-1198

Dr. Eugene C. Fischer (1)
Code 2840
Naval Surface Warfare Center
Carderock Division Detachment
Annapolis, MD 21402-1198

Defense Technical Information
Center (2)
Building 5, Cameron Station
Alexandria, VA 22314

* Number of copies to forward